J Mater Sci (2008) 43:568–572
DOI 10.1007/s10853-007-1702-y

Effects of non-uniform size distribution on the spectral optical gain properties of InGaAs/InGaAsP quantum dots

Jose Roberto Mialichi · Newton C. Frateschi

Received: 26 January 2007 / Accepted: 16 March 2007 / Published online: 12 June 2007

Abstract We present a theoretical study of the optical gain, emission wavelength, and threshold current density for edge emitting laser structures with an active region based on InGaAs/InGaAsP quantum dots. The analysis of the effects of the size distribution of the dots is also presented. Spectral gain curves are generated for InGaAs/InGaAsP dots where high optical gain and high independence of spectral characteristics are obtained for a uniform distribution of dots. With typical non-uniform distribution, we show a reduction in gain by a factor of 6. Also, we predict the onset of new transition peaks and a red shift in the most probable operating lasing wavelength. Finally, we demonstrate that there is a large range of full width at half maximum (FWHM) of the dots size distribution where variations in the maximum gain and associated wavelength, as well as threshold current density, are minimum.

Introduction

Nanostructures in active regions of lasers can provide an efficient mechanism for stimulated emission in both conventional Fabry–Perot lasers and non-conventional microresonator lasers. The insertion of 2D nanostructures, such as quantum wells, in the active region of semiconductors lasers has already allowed the use of quantum levels with the control of the emission wavelength through geometric characteristics of the structure [1]. Moreover, these structures have shown to provide greater gain and higher spectral purity. Also, one obtains a reduction in threshold current density due to larger spectral pumping concentration. In the last two decades, several efforts have concentrated in obtaining devices with nanostructured active region in the form of wires and dots [2]. With a complete dimensional reduction, such as for quantum dots, the creation of new active media in which not only complete control of the emission, but also its spectral properties dependence with carrier injection, are expected. A major problem towards obtaining these structures is the fact that quantum dots are obtained by self-assembled techniques where the control of uniformity of the dot size is very difficult [3].

In this work we describe an approach for the optical gain calculation of quantum dots [4], including the effects of the non-uniformity distribution of the dot's sizes for the application in laser structures. The wave function calculation is based on cylindrical geometry where the dots are treated as nanodisks in an approach similar to the one used for microdisk laser structures [5]. The insertion of these nanostructures in semiconductor laser active region is also considered for the investigation of the behavior of wavelength emission and threshold current density with the FWHM parameter inherent to the non-uniformity of the dots.

Optical gain applied in quantum dots

Based on the time-dependant perturbation theory, optical gain involving transitions between states in the conduction and valence band of direct bandgap semiconductors

J. R. Mialichi (✉) · N. C. Frateschi
Gleb Wataghin Physics Institute, State University of Campinas, DFA/LPD, CP 6165, Campinas, SP 13083-970, Brazil
e-mail: mialichi@ifi.unicamp.br

N. C. Frateschi
e-mail: fratesch@ifi.unicamp.br

can be given by a summation in the first Brillouin zone [6]:

$$g(E_f, E_{FC}, E_{FV}) = C(E_f) \int\int\int\int\int\int |M_{12}|^2 f_2(E_C, F_{EC})(1 - f_1(E_V, F_{EV}))\delta(E - E_f)\rho(\vec{k}_C)\rho(\vec{k}_V)\mathrm{d}^3\vec{k}_C\,\mathrm{d}^3\vec{k}_V \quad (1)$$

where E_f is the photon energy, E_C (E_V) is the conduction band energy level (valence band energy level), E_{FC} (E_{FV}) is the conduction quasi-Fermi level (valence quasi-Fermi level), $C(E_f) = \frac{\pi q^2 \hbar}{m_0^2 \varepsilon_0 E_f v_g}$, M_{12} is the transition matrix between the states, $\rho(\vec{k}_C)$, $\rho(\vec{k}_V)$ are density of states (conduction and valence bands) and f_1,f_2 are Fermi occupation probability for the valence and conduction bands, respectively. Considering parabolic bands and only direct transitions (k selection rule), and the case of quantum dots, the integrals in k-space are substituted by sums over all energy levels for each quantized dimensions. The optical gain is then given by:

$$g_{dot}(E_f, E_{FC}, E_{FV}) = C(E_f) \sum_{i,j,k}^{L,M,N} \left[\left| M_{dot}\left(E_{Ci,j,k}, E_{Vi,j,k}\right) \right|^2 \cdot \left[f_1\left(E_{Vi,j,k}, F_{EV}\right) + f_2\left(E_{Ci,j,k}, F_{EC}\right) - 1 \right] \cdot \rho_{dot} \right] \quad (2)$$

where the transition matrix and density of states are given by:

$$|M_{dot}|^2 = \frac{m^2 E^2}{\hbar^2} \left| \left\langle \Psi_{Cl,m,n}\left(E_{Cl,m,n}\right) \left| \hat{e} \cdot \vec{X} \right| \Psi_{Vl,m,n}\left(E_{Vl,m,n}\right) \right\rangle \right|^2 \quad (3)$$

$$\rho_{dot} = 2 \cdot N_{dot} \quad (4)$$

where $\hat{e} \cdot \vec{X}$ is the electric dipole operator. The literature refers to superficial density of dots of magnitude 1×10^{10} cm^{-2} [7]; we have used this value to estimate a volumetric density (N_{dot}) of 1×10^{15} cm^{-3}. The transition matrix is the electric dipole overlap between conduction eigenstate and valence eigenstate of the quantum dot Γ_{lmn} with the quantum numbers l,m, and n, respectively. The electric field is assumed to be in the radial direction of the nanodisk as shown in Fig. 1.

The calculation of the eigenstates and energy levels for quantum dots was obtained assuming the nanodisk approach where the thickness is much smaller than the radius. This is the case for many self-assembled structures. The quasi-Fermi levels for an electron hole density of $N_{e,h}$ can be given by:

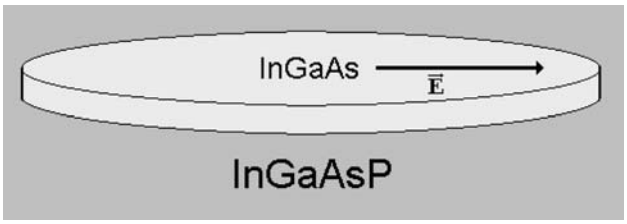

Fig. 1 The nanodisk approach was used to describe the form of the dot. Notice the direction of the electric field along the plane of the nanodisk

$$N_{e,h} = \left[\sum_{i,j,k}^{L_{C,v},M_{C,v}N_{C,v}} 2 \cdot N_{dot} \left(\frac{1}{e^{\left(E_{C,V(i,j,k)} - E_{Fc,v}\right)/kT} + 1} \right) \right] + \frac{1}{2\pi^2} \left(\frac{2m_{c,v}}{\hbar^2} \right)^{3/2} \int_{E_{C,Vmax}}^{\infty} E_{C,V}^{1/2} \left(\frac{1}{e^{\left(E_{C,V} - E_{Fc,v}\right)/kT} + 1} \right) \mathrm{d}E_{C,V} \quad (5)$$

where m is the effective mass of each band and $E_{max}$is the well depth. Sub-indices c, v refer to electrons or holes, respectively. To simplify our calculations, we consider the electron and hole densities to be equal. The injected carriers require a relaxation time to thermalize with the carriers in a quasi-equilibrium situation [8] by intraband scattering. We consider a Lorentzian distribution accounting for the intraband scattering.

Gaussian distribution of dots' dimensions

As found in the literature, quantum dots usually present a symmetrical distribution of sizes [9, 10]. We propose a Gaussian function to describe the distribution of radius dimension around 25 nm and we suppose the thickness constant and equal to 5 nm. We inserted a Gaussian distribution in Eq. 2 to obtain:

$$g_{dot_{Gaussian}}(E_f, N) = \int_0^{\infty} g_{dot}(E_f, N) G(R) \mathrm{d}r \quad (6)$$

where

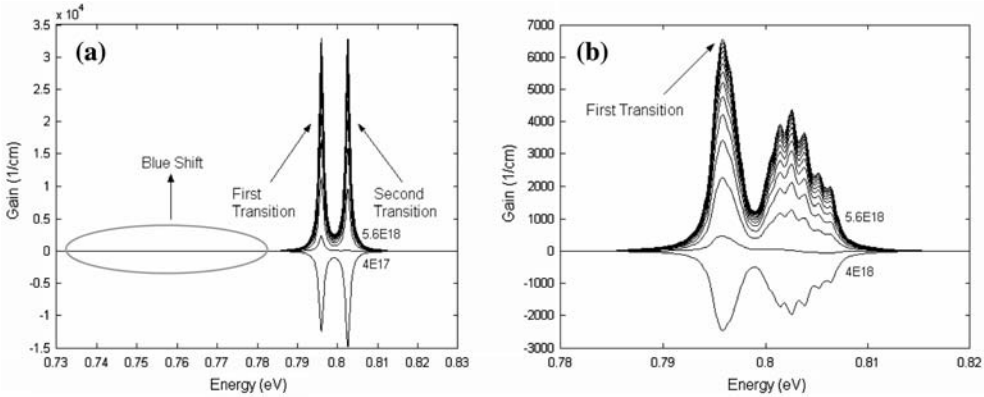

Fig. 2 Spectral gain curves for quantum dot in approximation to nanodisk (5 nm of thickness and 25 nm of radius)—InGaAs/InGaAsP system. (**a**) Homogeneous distribution of dots' dimensions. (**b**) Gaussian distribution of dots' dimensions with 7 nm FWHM

$$G(R) = \frac{1}{\sigma\sqrt{2\pi}} e^{-\frac{(R-\bar{R})^2}{2\sigma^2}} \tag{7}$$

Spectral gain curves

Figure 2 shows the calculated spectral gain curves generated by Eqs. 2 and 6 for carrier concentrations in a range between 4×10^{17} and 5.6×10^{18} 1/cm^3 in steps of 4×10^{17} 1/cm^3. The nanodots are considered to be made of InGaAs ($Q = 1.69$ μm) surrounded by InGaAsP ($Q = 1.41$ μm) material. Here, Q stands for the room temperature unstrained bandgap for the InP lattice matched compound. We have assumed $T = 300$ K; with a refractive index $n_{\text{InGaAs}} = 3.4548$; InGaAsP (InGaAs) conduction band effective mass of $m_{\text{C InGaAsP}} = 0.066m_0$ ($m_{\text{C InGaAs}} = 0.054\ m_0$); InGaAsP (InGaAs) valence band effective mass of $m_{\text{hhInGaAsP}} = 0.489m_0$ ($m_{\text{hhInGaAs}} = 0.447m_0$).

The spectral gain curves in Fig. 2a show two peaks corresponding to the allowed nanodisk energy transitions. Obviously, the quantum dot levels are discrete with a discrete density of states. Therefore, the line-width of each transition is completely controlled by intraband scattering time. The gain increases as carrier concentration increases since the quasi Fermi levels are becoming more separated. The gain becomes positive for concentrations values above 4.0×10^{17} 1/cm^3. For energies below the first transition energy of the dot, the semiconductor becomes transparent. In other words, there is a blue shift of ~0.79 eV with respect to the bandgap energy of InGaAs (0.73 eV). Figure 2b shows the spectral gain for the same structures depicted in Fig. 2a, but with a Gaussian distribution of the nanodisk's radius with FWHM of 7 nm. A preliminary analysis shows that the gain values reduce significantly (over six times) when we consider the Gaussian distribution. Also, it is possible to observe the presence of new energy levels related to the variation of the nanodisk radius. Therefore, both gain and the spectral purity are seriously affected by the presence of non-uniformity in the dot's sizes.

It is interesting to compare the gain and spectra dependence with carrier concentration for the uniform and non-uniform size distribution. Figure 3a shows the maximum optical gain as a function carrier concentration. Figure 3b shows the maximum optical gain as a function of the wavelength where it occurs for the different carrier concentrations. Clearly gain reduction is observed as expected. On the other hand, for both cases, wavelength insensitivity to carrier concentration is observed.

Notice that even though the wavelength remains unchanged for different values of concentration, there is a red shift with respect to the uniform dot distribution as

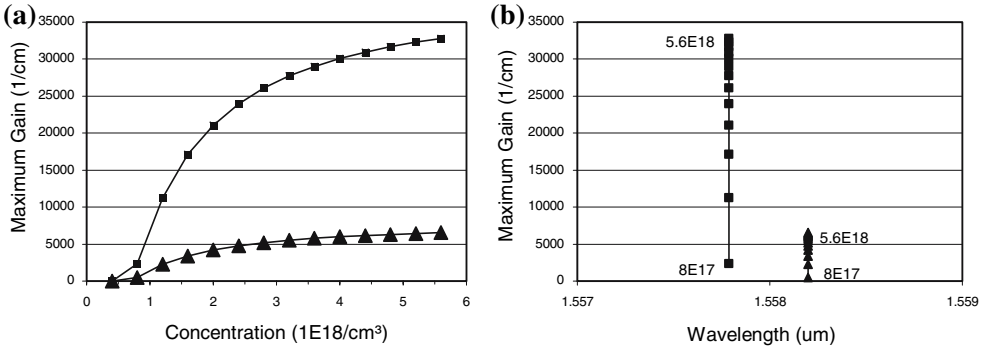

Fig. 3 Square refers to homogeneous distribution and triangle refers to Gaussian distribution. (**a**) The maximum gain obtained in the spectral curves of Fig. 2 are plotted with respect to carrier concentration. (**b**) The maximum gain obtained for the spectral curves of Fig. 2 are plotted with respect to the corresponding wavelength where the maximum occurs

shown in Fig. 3b. This effect can be explained by the fact that the variation of the nanodisk radius allows the presence of lower energy levels that in general will be the first levels to provide gain. This result shows that the choice of the desired wavelength must be preceded by the knowledge of the inherent parameters of the Gaussian distribution.

Dependence with FWHM

Spectral gain curves were calculated for distribution of dots with different values of FWHM. We consider only the first transition and one carrier concentration of 5.6×10^{18} 1/cm^3. The same values of dots' dimensions (5 nm of thickness and 25 nm of average radius) and InGaAs/InGaAsP system parameters are used. The maximum gain and its associated wavelength are plotted as a function of the radius FWHM in Fig. 4.

Figure 4a shows an approximately constant value for the maximum gain for 4 nm < FWHM < 15 nm. The larger gain value for the smaller FWHM is related to the higher spectral density that exists given the reduction in the number of available energy levels. In fact, as shown above, the maximum gain tends to increase up to six times from a non-uniform to a uniform distribution. As the FWHM becomes higher than 15 nm a large reduction in maximum gain is obvious. At this point, the onset of more confined levels increases the density of states, reducing the quasi-Fermi level variation with injected carrier concentration. Figure 4b shows that the first transition has a large red shift exactly at this value corroborating with our hypothesis. Therefore, as the FWHM increases, one should expect a step like curve for both the maximum gain and the associated wavelength due to the onset of new allowed transitions.

Although the operating wavelength depends on the Gaussian distribution properties, the interval 4–13 nm in FWHM provides an ideal region with both maximum gain and wavelength emission remain constant. Therefore, the above FWHM range should be targeted for the synthesis of dots if predictability in laser threshold current density or emission wavelength is desired. Also, the FWHM has to be definitely kept below 15 nm. Obviously, these limit values will depend on the average radius, but since we are using typical dots sizes reported in the literature, these numbers are a good example.

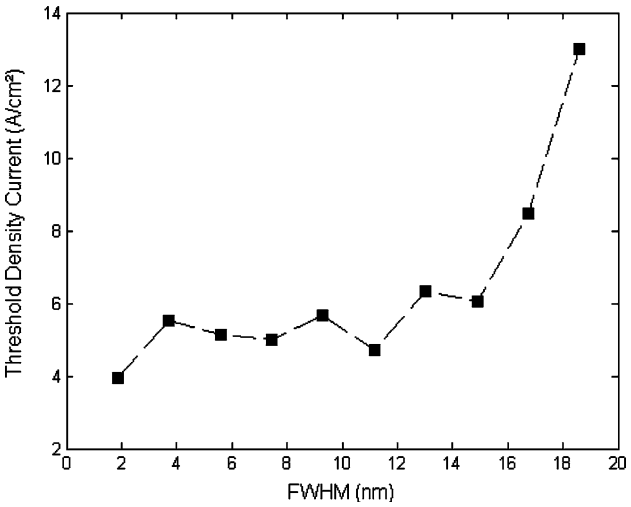

Fig. 5 The threshold current density associated to the first transition for different values of FWHM, are plotted with respect to this values

At this point it is interesting to evaluate the effects of the non-uniform distribution in a typical edge emitting laser structure [11]. The threshold condition occurs when the modal gain reaches the total optical loss [12]:

$$\Gamma g(E, n_{\text{th}}) = \alpha_i + \frac{1}{L}\ln\left(\frac{1}{r}\right) \tag{7}$$

where α_i is the optical internal loss, here assumed to be 10 cm^{-1}; Γ is the confinement factor of 0.007, in our case; r is the reflectivity, assumed of 0.3; and L is a laser length of 750 μm. We consider a laser waveguide width of 4 μm. From Eq. 7, the threshold current density is easily obtained as $J_{\text{th}} = e(Bn_{\text{th}}^2 + Cn_{\text{th}}^3)\cdot t$, where n_{th} is the threshold carrier density, t is the thickness of the dots, B is spontaneous recombination rate of 10^{-10} cm^3/s and C is Auger recombination coefficient of 10^{-29} cm^6/s [6]. Figure 5 shows the threshold current density (J_{th}) dependence with FWHM.

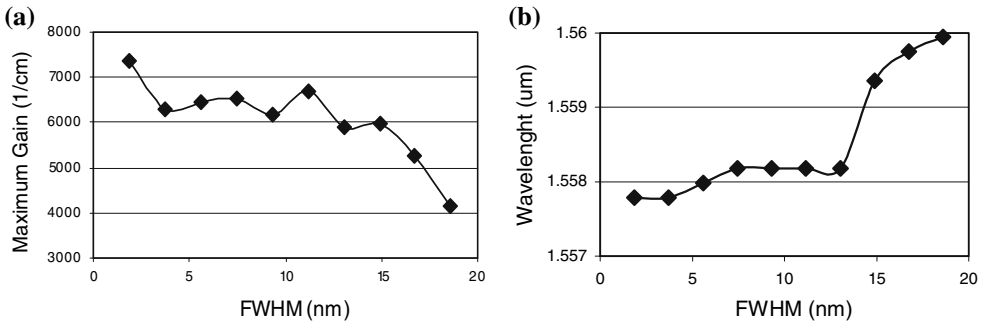

Fig. 4 (**a**) Maximum gain versus FWHM. (**b**) The Maximum gain wavelength versus FWHM

We have considered only the first transition frequency of each FWHM spectral gain curve.

Obviously, Fig. 5 presents the inverse behavior of Fig. 4a since J_{th} depends directly on the optical gain. Similar to Fig. 4a, J_{th} remains approximately constant at 5.8 A/cm^2 between 4 and 15 nm of FWHM and a subsequent deterioration of J_{th} for values of FWHM > 15 nm is clearly observed. The corresponding threshold current (I_{th}) for J_{th} equal to 5.8 A/cm^2 is approximately 0.2 mA. In fact, the small volume combined with the efficient mechanism of stimulated emission of the nanodots provide low values of lasing operating current.

Conclusion

We present a theoretical calculation of the optical gain in quantum dots based on InGaAs/InGaAsP material. High gain at discrete levels with linewidth limited by intraband scattering is obtained. Also, higher maximum gain independence with carrier concentration is observed for a uniform dot distribution. With a non-uniform distribution, despite the wavelength insensitivity to changes in carrier concentration, we show a reduction in gain by a factor of 6, the onset of new transition peaks and a red shift in the most probable lasing operating wavelength. In both cases the wavelength at maximum gain remains unchanged for different values of carrier concentration. The maximum gain and wavelength emission dependence with FWHM shows that a range between 4 and 13 nm is desirable for dots with average radius of 25 nm. Also, we show great deterioration in performance for FWHM above 15 nm. These are targets to be aimed when optimizing the conditions for the synthesis of the quantum dots if they are intended to be used in the active region of semiconductor lasers.

Acknowledgments Authors would like to acknowledge National Council for Research and Development (CNPQ) and State of Sao Paulo foundation for the support of research (FAPESP) for the financial support.

References

1. Thijs PJA, Tiemeijer LF, Binsma JJM, van Dongen T (1994) IEEE J Quantum Electron 30:477
2. Nì AC, Poole PJ, Marshall P, Fraser J, Raymond S, Fafard S (2002) Appl Phys Lett 80:3629
3. Xua B et al (2004) IEEE 13th international conference on semiconducting and insulating materials, p 113
4. Kovsh AR, Zhukov AE, Egorov AY, Ustinov VM, Ledentsov NN, Maksimov MV, Tsatsul'nikov AF, Kop'ev PS (1999) Semiconductors 33(2):184
5. Frateschi NC, Levi AFJ (1996) J Appl Phys 80:644
6. Agraval GP, Dutta NK (1993) Semiconductor lasers. Van Nostrand, Reinhold
7. Leonard D, Fafard S, Pond K, Zhang YH, Merz JL, Petroff PM (1994) J Vac Sci Technol B 12(4):2516
8. Yamada M, Ishiguro H, Nagato H (1980) Jap J Appl Phys 19:135
9. Mendoza-Alvarez JG, Pires MP, Landi SM, Lopes AS, Souza PL, Villas-Boas JM, Studart N (2006) Physica E 32(1–2):85
10. Sormunen J, Riikonen J, Mattila M, Sopanen M, Lipsanen H (2005) Nanotechnology 16:1630
11. Reithmaier JP et al (2005) J Phys D: Appl Phys 38:2088
12. Coldren LA, Corzine SW (1995) Diode lasers and photonic integrated circuits. Wiley, New York